Experimental Eye Research 137 (2015) 111–124

Contents lists available at ScienceDirect

Experimental Eye Research

journal homepage: www.elsevier.com/locate/yexer

Review

Rabbit as an animal model for intravitreal pharmacokinetics: Clinical predictability and quality of the published data

Eva M. del Amo [a, b], Arto Urtti [a, b, *]

[a] School of Pharmacy, University of Eastern Finland, Kuopio, Finland
[b] Centre for Drug Research, Division of Pharmaceutical Biosciences, Faculty of Pharmacy, University of Helsinki, Finland

ARTICLE INFO

Article history:
Received 5 March 2015
Received in revised form
7 May 2015
Accepted in revised form 10 May 2015
Available online 12 May 2015

Keywords:
Ocular pharmacokinetics
Drug delivery
Intravitreal
Animal model
Rabbit

ABSTRACT

Intravitreal administration is the method of choice in drug delivery to the retina and/or choroid. Rabbit is the most commonly used animal species in intravitreal pharmacokinetics, but it has been criticized as being a poor model of human eye. The critique is based on some anatomical differences, properties of the vitreous humor, and observed differences in drug concentrations in the anterior chamber after intravitreal injections. We have systematically analyzed all published information on intravitreal pharmacokinetics in the rabbit and human eye. The analysis revealed major problems in the design of the pharmacokinetic studies. In this review we provide advice for study design. Overall, the pharmacokinetic parameters (clearance, volume of distribution, half-life) in the human and rabbit eye have good correlation and comparable absolute values. Therefore, reliable rabbit-to-man translation of intravitreal pharmacokinetics should be feasible. The relevant anatomical and physiological parameters in rabbit and man show only small differences. Furthermore, the claimed discrepancy between drug concentrations in the human and rabbit aqueous humor is not supported by the data analysis. Based on the available and properly conducted pharmacokinetic studies, the differences in the vitreous structure in rabbits and human patients do not lead to significant pharmacokinetic differences. This review is the first step towards inter-species translation of intravitreal pharmacokinetics. More information is still needed to dissect the roles of drug delivery systems, disease states, age and ocular manipulation on the intravitreal pharmacokinetics in rabbit and man. Anyway, the published data and the derived pharmacokinetic parameters indicate that the rabbit is a useful animal model in intravitreal pharmacokinetics.

1. Introduction

Age-related macular degeneration, glaucoma, diabetes, and various rare ocular diseases may impair the functionality of the retina leading to visual impairment and blindness. Even though this is a growing problem in the aging populations, effective treatments are not available to most patients with retinal diseases.

New mechanisms of action and drug candidates are being discovered for the retinal diseases (Zhang et al., 2012), but drug delivery to the retina is very difficult (and often impossible) from topical eye drops or systemic medications (such as tablets). Therefore, the intravitreal injections have emerged as the primary method of drug administration to the retina and choroid (del Amo and Urtti, 2008; Urtti, 2006). The number of annual intravitreal injections has increased rapidly being nearly 400,000 in the United Kingdom (Severn and Hamilton, 2015) and probably an order of magnitude higher numbers in Europe and U.S.A. For example, bevacizumab (Avastin®), ranibizumab (Lucentis®), pegaptanib sodium (Macugen®), aflibercept (Eylea®) and triamcinolone acetonide (Kenalog®) are widely used as intravitreal injections to treat neo-vascular macular degeneration and other retinal diseases.

ABBREVIATIONS: AIC, Akaike's information criterion; AUC, area under the curve; C_0, drug concentration at time zero; C_{calc}, calculated concentration; CL_{ivt}, intravitreal clearance; CL_{RPE}, intravitreal clearance across the RPE; C_{obs}, observed concentration; CV%, coefficient of variation; D_{ivt}, intravitreal dose; E, extraction ratio; $k_{elimination}$, first-order elimination rate constant; $f_{u,\ vitreous}$, fraction of unbound drug in vitreous; $f_{u,\ tissue}$, fraction of unbound drug in the tissue; K_p, distribution coefficient between the tissue and vitreous; MW, molecular weight; P, permeability in the membrane; ρ, Spearman's rank correlation coefficient; R^2, coefficient of determination; Q, flow; RPE, retinal pigment epithelium; S, membrane surface area; $t_{1/2,\ ivt}$, intravitreal half-life; TEER, trans-epithelial electrical resistance; V, anatomical tissue volume; $V_{ss,\ ivt}$, intravitreal volume of distribution; Y, actual concentration; Y hat, predicted concentration.

* Corresponding author. School of Pharmacy, University of Eastern Finland, P.O. Box 1627, 70211 Kuopio, Finland.
E-mail address: arto.urtti@uef.fi (A. Urtti).

http://dx.doi.org/10.1016/j.exer.2015.05.003

Intravitreal injection is an invasive procedure and, therefore, the dosing intervals should be long. The dosing intervals of intravitreal injections of antibodies, aptamers, soluble receptors and suspensions are often four to six weeks and sometimes even twelve weeks (Bashshur et al., 2008; Cheung and Eaton, 2013). This is based on the slow clearance, long half-life (about two to six days) and extremely high potency the macromolecules (anti-VEGF antibodies and soluble receptors) or slow dissolution and long residence time of suspension particles (corticosteroid suspensions). However, in the case of intravitreal solutions of small molecular drugs, the fast elimination rates (half-lives of 1–27 h) would lead to frequently repeated injections that are not possible in the clinical setting. Moreover, injections of the drug solutions intravitreally lead to high fluctuations in intravitreal drug concentrations. This is feasible only for the drugs with wide therapeutic index, otherwise the adverse effects would prohibit the clinical use. Controlled release formulations can maintain the intravitreal drug concentrations within the therapeutic index for prolonged periods, thereby allowing long dosing intervals of several months. Some controlled release implants are already in the clinical use for instance, fluocinolone acetonide intravitreal implant (Iluvien®) and dexamethasone intravitreal implant (Ozurdex®) (del Amo and Urtti, 2008; Sanford, 2013; Totan et al., 2015). Estimation of the time course of drug effects in the posterior eye segment is possible with pharmacokinetic modeling tools (Kontturi et al., 2014; Stewart and Rosenfeld, 2008).

After intravitreal administration, drugs distribute to the ocular tissues (lens, iris, ciliary body, retina). Distribution depends on the ability of drug to partition into the tissues and it is described as volume of drug distribution. Drug elimination may take place posteriorly through the blood-retina barrier (Duvvuri et al., 2003; Gupta et al., 2000; Maurice and Mishima, 1984; Shen et al., 2007) to the choroidal blood circulation that constitutes most of the ocular blood flow (del Amo et al., 2015; Roh et al., 2006). Intravitreal drug is eliminated also anteriorly via aqueous humor turnover and uveal blood flow. The importance of anterior and posterior routes depends on the drug properties (Maurice and Mishima, 1984): lipophilic drugs with high permeability in the blood-retina barrier are mostly eliminated posteriorly (e.g. fluconazole; vitreal clearance 0.753 ml/h (Gupta et al., 2000)), whereas elimination of large and hydrophilic compounds is restricted to the anterior route (e.g. bevacizumab; vitreal clearance 0.019 ml/h (Bakri et al., 2007; Christoforidis et al., 2011; del Amo et al., 2015)). These processes determine drug elimination in rabbit and human eyes and it is described as intravitreal clearance. Ocular pharmacokinetic parameters (i.e. volume of distribution and clearance) are the most informative, reliable and quantitative basis for the pharmacokinetic comparisons in terms of species, disease states, age, drug compounds and delivery systems.

Ocular pharmacokinetics has only rarely been studied in the human eye, because the invasive sampling from the human eye is ethically restricted and may influence pharmacokinetics. Therefore, ocular pharmacokinetics relies on animal models, mostly rabbits. Recently, the rabbit eye has been criticized for being a poor model of the human eye (Laude et al., 2010; Rowe-Rendleman et al., 2014). Therefore, we investigated all available intravitreal pharmacokinetic data in rabbits (del Amo et al., 2015) and humans (this review) and derived the pharmacokinetic parameters (clearance, volume of distribution) to compare systematically intravitreal pharmacokinetics in man and rabbit. We did not find any convincing evidence to justify the criticism of the rabbit model. Moreover, during the process of analyzing the intravitreal pharmacokinetic parameters in the rabbit eyes (del Amo et al., 2015), we noticed another remarkable problem: many published studies are based on suboptimal study designs, and actually 58% of the studies were discarded from the pharmacokinetic data analysis.

In this review, we summarize the current knowledge of intravitreal pharmacokinetics in rabbits and humans, and provide advice in intravitreal pharmacokinetic study design.

2. Intravitreal pharmacokinetics in rabbit eye

2.1. Introduction of concepts

The intravitreal pharmacokinetics is defined by the primary parameters: volume of distribution ($V_{ss,\ ivt}$) and clearance (CL_{ivt}) that describe drug distribution and elimination, respectively.

$V_{ss,\ ivt}$ can be compared to the anatomical volumes of the ocular tissues based on the principles from the drug distribution from plasma to the tissues (Jusko, 2006; Mager, 2006):

$$V_{ss,\ ivt} = V_{vitreous} + V_{lens} \times K_{p,\ lens} + V_{ciliary\ body} \times K_{p,\ ciliary\ body} + V_{retina} \times K_{p,\ retina} \cdots \quad (1)$$

where V values indicate the anatomical tissue volumes and K_p distribution coefficients of the drug between the tissue and vitreous. High K_p values indicate effective drug partitioning to the tissues, leading to $V_{ss,\ ivt}$ values bigger than the anatomical volumes.

Systemic volume of drug distribution at steady-state can be related to the anatomical volumes using Gillette equation (Gillette, 1971; Mager, 2006). In this case, the equation for the intravitreal drug delivery would be:

$$V_{ss,\ ivt} = V_{vitreous} + V_{lens} \times \frac{f_{u,\ vitreous}}{f_{u,\ lens}} + V_{ciliary\ body} \times \frac{f_{u,\ vitreous}}{f_{u,\ ciliary\ body}} + V_{retina} \times \frac{f_{u,\ vitreous}}{f_{u,\ retina}} \cdots \quad (2)$$

where V values indicate the anatomical tissue volumes and f_u terms indicate the fractions of unbound drug in the vitreous and surrounding tissues. Thus, in the context of intravitreal administration, $V_{ss,\ ivt}$ is related to the anatomical volumes ($V_{vitreous}$, $V_{tissues}$) and either 1) drug distribution between the tissues and vitreous humor (K_p) or 2) free fractions of the drug in the vitreous ($f_{u,\ vitreous}$) and tissues ($f_{u,\ tissue}$). Anyway, in both cases, high drug concentrations in the tissues increase the value of $V_{ss,\ ivt}$.

CL_{ivt} can be related to the ocular flows:

$$CL_{ivt} = Q_{ocular} \times E_{ocular} \quad (3)$$

where Q is the ocular flow and E is the extraction ratio in the tissue ($0 < E < 1$). Theoretical maximum for CL_{ivt} is equal to the ocular flows (aqueous humor and blood flows) representing completely flow-limited clearance without any membrane barrier limitations (e.g. blood-retinal barrier). On the contrary, at low values of E the clearance is limited by membrane permeation and defined as product of drug permeability in the membrane (P) and the membrane surface area (S):

$$CL_{ivt} = P_{ocular\ barriers} \times S_{ocular\ barriers} \quad (4)$$

After intravitreal injection, the drug is partitioning to some extent to the surrounding tissues and eliminated from the vitreous through aqueous humor turnover and blood-ocular barriers (Fig. 1). Membrane permeable drugs can cross the blood-ocular barriers, while poorly permeable drugs (e.g. macromolecules) will be cleared via aqueous humor turnover (Maurice and Mishima, 1984). All intravitreal drug will eventually end-up to the systemic

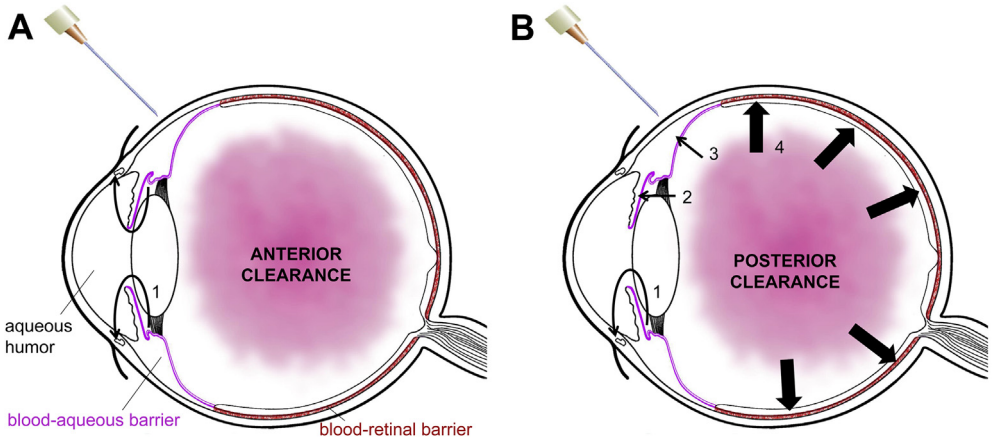

Fig. 1. Routes of drug elimination after intravitreal injection. (A) Anterior elimination of the drug in the aqueous humor flow (1). (B) Drug elimination through blood-ocular barriers. The drug permeates through the posterior iris epithelium into iris vein and is drained by vortex veins (2), through the non-pigmented ciliary epithelium to ciliary muscles and from the ciliary plexus to the episcleral veins (3), to the retinal capillaries and through the retinal pigment epithelium (RPE) into the choroid and systemic circulation (4) (del Amo et al., 2015).

circulation unless it is metabolized in the eye which is not habitual fate. However, the systemic circulation can be handled as a sink because the clearance in the human systemic circulation is much higher (10–100,000 ml/h) than the clearance in the eye (0.01–1.0 ml/h). Therefore, the concentrations in the systemic circulation are orders of magnitude lower than in the eye, and drug elimination from the eye is rate-limited by the ocular processes, and not affected by the drug concentrations in the blood circulation.

The primary pharmacokinetic parameters $V_{ss,\ ivt}$ and CL_{ivt} are useful in pharmacokinetic simulations and clinical translation. They allow estimation of average steady-state concentrations, concentration profiles, half-life ($t_{1/2,\ ivt}$) and amount of drug in the eye after administration of different doses or dosage forms (del Amo et al., 2015). $V_{ss,\ ivt}$ and CL_{ivt} can be linked to the fundamental factors, anatomy, physiology, and drug interactions with tissues, thereby providing understanding of ocular pharmacokinetics in the physiological context and generating tools for bottom-up simulation models (del Amo et al., 2015). Noteworthy, the most frequently used intravitreal pharmacokinetic parameter, $t_{1/2,\ ivt}$ depends on both drug distribution and elimination,

$$t_{1/2,\ ivt} = \frac{ln2 \times V_{ss,\ ivt}}{CL_{ivt}} \quad (5)$$

if the intravitreal concentration profile shows multi-exponential decline, the $t_{1/2,\ ivt}$ correspond to effective $t_{1/2,\ ivt}$. Even though $t_{1/2,\ ivt}$ is useful in defining the dosage intervals of the drug, it does not allow mechanistic analyses and simulations. Half-life cannot be linked to physiology and pathophysiological alterations in the eye.

2.2. Analysis of the literature

Recently, we developed a universal collection of $V_{ss,\ ivt}$, CL_{ivt} and $t_{1/2,\ ivt}$ values (del Amo et al., 2015). For that, we carried out a comprehensive literature search on intravitreal pharmacokinetic studies in healthy and normal rabbit eyes during 1947–2013. We set criteria for the data quality: at least four time-points, at least two replicates per point, and balanced sampling for at least a time-span of two $t_{1/2,\ ivt}$ of the drug (the derived parameters values are presented later in the Section 2.4). The criteria are needed for reliable determination of $V_{ss,\ ivt}$, CL_{ivt} and $t_{1/2,\ ivt}$ values. Surprisingly, only 42% of the literature reports fulfilled these quality criteria. The corresponding references and the data analysis are presented in our previous paper (del Amo et al., 2015). The remaining 58% (92 reports) had to be discarded due to inadequate data points or other problems (e.g. analytical issues, poor match between dose and initial concentration, solubility problems) that prevent reliable data analysis. Commonly, the problems were related to inadequate number of data points, poorly selected time spans and narrow concentration ranges. Table 1 illustrates some data quality problems that hamper the calculation of the pharmacokinetic parameters ($V_{ss,\ ivt}$, CL_{ivt} and $t_{1/2,\ ivt}$) or lead to unreliable estimates. For the analysis *Phoenix WinNonlin® software* (*version 6.3, Pharsight Inc., St. Louis, USA*) was used and accurate description of the workflow is described in Section 2.3.

Even though many intravitreal pharmacokinetic studies did not meet the normal quality standards, they give rough estimates of $t_{1/2,\ ivt}$ and range of drug concentrations after injection of a certain dose. Such information is valuable and important, but unfortunately not adequate for determination of pharmacokinetic parameters accurately.

2.3. Design of an intravitreal pharmacokinetic study

In a typical intravitreal pharmacokinetic study, drug is injected into the vitreal cavity in rabbits and, thereafter, drug concentrations are determined periodically. In most studies, the animals are sacrificed at different time intervals: the eyes are removed and the vitreous humor samples are assayed for drug concentrations. Continuous sampling with a microdialysis probe in the rabbit eyes has also been used (Atluri and Mitra, 2003). This approach reduces the number of animals, but reliable recovery estimates are needed in the determination of the drug yield (Duvvuri et al., 2003) and the duration of the experiments is often limited. In some cases, a radioactively labeled drug has been injected to the vitreous followed by imaging with positron emission tomography (Christoforidis et al., 2011, 2012). In all cases, the sampling times are crucial for obtaining reliable pharmacokinetic profiles and parameter values.

In rabbit studies, the number of test animals should be minimized based on 3R (Reduce, Refine, Replace) principles, but this should not lead to inadequate experimental design, unreliable pharmacokinetic profiles and parameters (Section 2.2.). Good practices of systemic pharmacokinetic data analyses should be applied with some modifications in ocular pharmacokinetics. The

Table 1
Typical examples of intravitreal data that cannot be used for reliable estimation of pharmacokinetic parameters are illustrated. These literature data were used for parameter estimation with Phoenix software following the advice from Section 2.3. The calculation of the estimated concentration at time 0 (C_0) is based on 1.15 ml rabbit vitreous volume (del Amo et al., 2015).

Missing initial data points	Missing intermediate data points	Missing data points in the terminal phase	Lack of adequate data points	Too short duration of the study
Candesartan (Lee et al. 2011) Dose = 1000 μg Estimated $C_0 \approx$ 870 μg/ml Albino rabbit	Moxifloxacin (Iyer et al. 2006) Dose = 200 μg Estimated $C_0 \approx$ 174 μg/ml Pigmented rabbit	Diclofenac (Durairaj et al. 2009) Equivalent dose = 279 μg Estimated $C_0 \approx$ 243 μg/ml Albino rabbit	Bevacizumab (Nomoto et al. 2009) Dose = 1250μg Estimated $C_0 \approx$ 1087 μg/ml Pigmented rabbit	Acyclovir (Hughes et al. 1996) Dose = 200 μg Estimated $C_0 \approx$ 174 μg/ml Pigmented rabbit
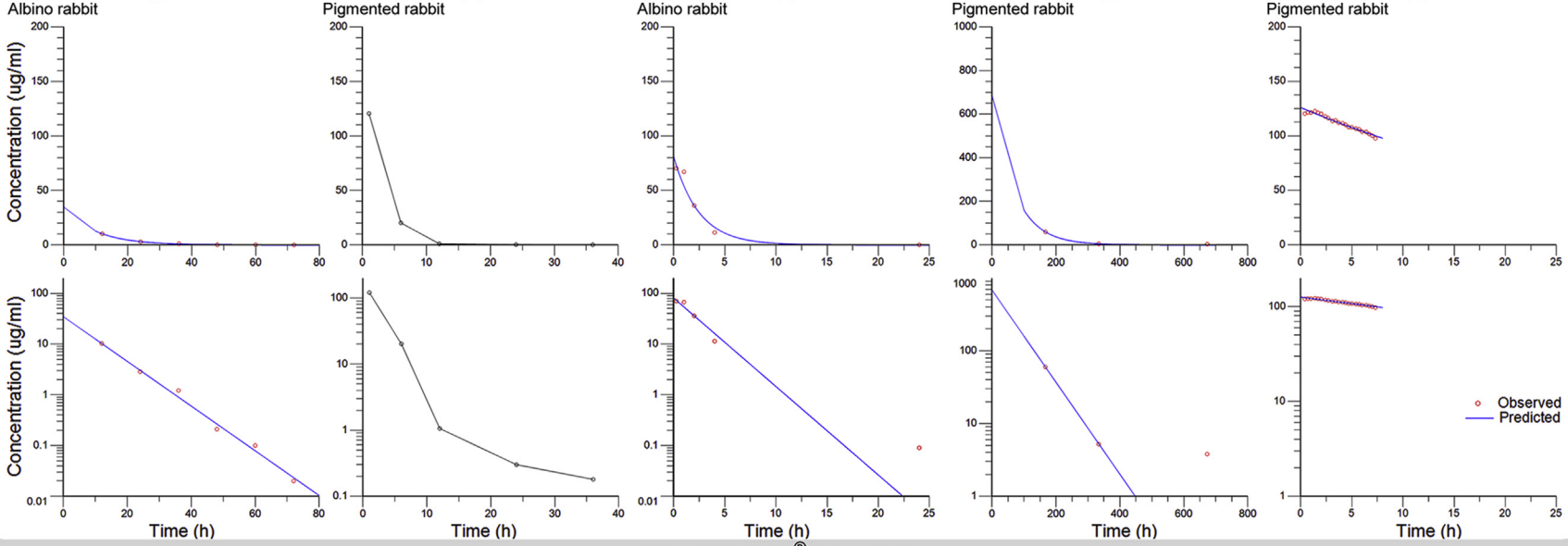				
Phoenix WinNonlin® data analysis				
One-compartment model with uniform weighting gave unrealistic parameter values: $V_{ss,ivt}$ = 28 ml, CL_{ivt} = 2.92 ml/h that were outside the range in the big data set [a] Correlation between parameters > 0.95 (unacceptable) The first sample is 1.2 % of the concentration at time zero. Most drug (98.8%) was eliminated before the first sample. Not enough initial data points for compartmental model fitting.	One- and two-compartmental analyses failed to fit the data. Not enough intermediate data points for compartmental model fitting.	One-compartment model with 1/Yhat weighting gave: $V_{ss,ivt}$ = 3.72 ml and CL_{ivt} = 1.494 ml/h (doubtful values comparing with the range[a]) It appears that the drug obeys two-compartmental kinetics, since the last data point is far above the fitted line. The single data point in the terminal elimination phase does not allow proper analysis with two-compartmental model. The last data point has too big role and this involves high risk of error. Not enough data points at the terminal phase for compartmental model fitting.	One-compartment model with uniform weighting. Correlation between parameters >0.95 (unacceptable); CV% > 30% (unacceptable); negative confidence intervals (unacceptable). Not enough data points for reliable compartment model fitting.	One-compartment model with uniform weighting gave: $V_{ss,ivt}$ = 1.59 ml and CL_{ivt} = 0.05 ml/h (unreliable value). The statistics were within the acceptable limits. However, the sampling time in this microdialysis study was too short and it did not allow reliable determination of the pharmacokinetic parameters. About 56% of the drug has not been eliminated at the time of the last sample. Not enough data points for reliable compartment model fitting.

a: The range values of $V_{ss,\ ivt}$ and CL_{ivt} in rabbit vitreous is 0.72–3.14 ml and 0.011–1.530 ml/h respectively (Fig. 2 and del Amo et al., 2015).

Table 2
Pharmacokinetic data analysis with curve fitting software.

Compartmental model
Select one- or two- compartmental model.
The experimental data are plotted in semi-logarithmic plot: logarithm of intravitreal concentration vs time.
Based on the shape of the plotted data one-compartmental (single slope) or two-compartmental (two distinct slopes) model may be feasible.
Weighting factor
Weighting is used to improve the curve fitting by giving more weight to the last data points with low concentrations.
The sum of squared residuals can be weighted by
• one (uniform weighting)
• $1/C_{obs}$ or $1/C_{calc}$ (1/Y or 1/Yhat respectively)
• $1/(C_{obs})^2$ or $1/(C_{calc})^2$ ($1/Y^2$ or $1/Yhat^2$ respectively)
The relative weight of small concentrations is increased with the use of the concentration or squared concentration in the denominator.
Y is the actual concentration and Yhat is the predicted concentration.
Goodness of fit
Goodness of fit describes how close the calculated curve is to the data points. The following criteria is used to evaluate the goodness of fit:
1) Calculated concentration curve should lie between the observed concentration points.
2) Signs of the residuals (i.e., $C_{obs} - C_{calc}$, shows either over-estimation or under-estimation) must change randomly. This indicates lack of systematic deviations.
3) Relative residuals (residual/C_{obs}) are not excessive at low concentrations.
4) Confidence intervals of the parameters are positive. This depends on the number of animals and data points, and the complexity of the pharmacokinetic model.
5) Coefficient of variation (CV%) should be less than 30%, preferably below 10%.
6) Correlation between various pharmacokinetic parameters should be < 0.95. This informs us that the parameters are independent from each other.
7) Sum of weighted squared residuals should be small enough.
8) Akaike's information criterion (AIC) is used to discriminate between models (for example, one- and two-compartment models) with the same weighting. The best model has the lowest AIC value.

pharmacokinetic parameters are determined using curve fitting software (e.g. *Kinetica®, Thermo Fisher Scientific Inc, Waltham, USA or Phoenix WinNonlin® software*) that are based on the method of least squares to fit the concentration curves. The objective is to minimize the difference between the observed and calculated concentrations (C_{obs} and C_{calc} respectively), *i.e.* sum of squared residuals $\Sigma(C_{obs} - C_{calc})^2$. These methods pool all the data from the experiment for maximal information gain. As illustrated in Table 1 inadequate data may not allow reliable estimation of pharmacokinetic parameters. Proper procedure in pharmacokinetic data analysis is presented in Table 2.

Usually, the kinetic analysis is done for each individual separately (e.g. plasma samples at different times), but this is not possible in intravitreal studies, because multiple sampling from the vitreous is not possible. All individual data points can be fitted simultaneously, and the fitted curve can be compared to the observed mean values or individual points. In any case, it is important to have adequate number of data points with proper time span and concentration range.

We propose that the following points should be taken into account in the design of intravitreal pharmacokinetic studies. Firstly, the drug dose should be soluble in the formulation and in the vitreous. This is not the case in many studies (some examples (Chin et al., 2005; Doft et al., 1985; Wingard et al., 1989)). Then, the resulting data does not allow reliable determination of CL_{ivt}, $V_{ss,\ ivt}$ and $t_{1/2,\ ivt}$ for the drug. Anyway, the obtained concentration profiles describe the properties of the formulation in drug delivery. Secondly, the dose should be reported, and if the drug is in salt form, the reporting should allow the estimation of dose as free acid or free base. Thirdly, at least six time points must be used at properly balanced intervals to describe drug distribution and elimination. The first data point should be shortly after injection and, thereafter, the data points should span at least three $t_{1/2,\ ivt}$ of the drug (*i.e.* at least 87% of the drug has been eliminated at that point). Fourthly, at least four to six replicate eyes should be used for each time point. Overall, this will results in 24–36 rabbit eyes (12–18 animals). Within the European Union the use of animals in scientific experiments should be rationally reduced (Directive 86/609/EEC). Properly conducted intravitreal pharmacokinetic study uses many rabbits, but it will yield reliable quantitation of pharmacokinetics (incl. $V_{ss,\ ivt}$, CL_{ivt}, $t_{1/2,\ ivt}$) that allows estimation of drug concentrations at different dosing regimens thereby reducing the need of animals in later experiments and in the long run.

2.4. Intravitreal pharmacokinetic parameters in rabbits

The universal collection of the intravitreal pharmacokinetic data in rabbits was followed by determination of the primary pharmacokinetic parameters (CL_{ivt} and $V_{ss,\ ivt}$). Only the studies that fulfilled the quality criteria were included in the analysis. The CL_{ivt} and $V_{ss,\ ivt}$ data are plotted against the molecular weight (MW) of the compounds in Fig. 2A–B.

The $V_{ss,\ ivt}$ values in rabbits are in the range 0.72–3.14 ml. Interestingly, there are no systematic differences in the $V_{ss,\ ivt}$ values of small molecules and macromolecules. Overall, the scope of $V_{ss,\ ivt}$ values is narrow (only 4-fold range) and in general the values are slightly greater than the anatomical volume of the vitreous humor (1.15 ml) (Fig. 2B). Volume of vitreous is bigger than the volumes of the surrounding tissues, such as iris, ciliary body, choroid, retina (0.050–0.059 ml) (Wiederholt et al., 1986; Wu et al., 1970) and lens (0.33–0.53 ml) (Zamudio and Candia, 2011). The small volumes of the tissues explain the narrow range of $V_{ss,\ ivt}$ values (see Eqs. (1) and (2)). The highest $V_{ss,\ ivt}$ value (3.14 ml) would be achieved with K_p (or $f_{u,\ vitreous}/f_{u,\ tissue}$) value of 2.8–4 if we use the average combined volume for the surrounding tissues (0.49–0.69 ml) in Eq. (1) or Eq. (2), proving that K_p values in the eye are moderate and do not have major impact on $V_{ss,\ ivt}$ values. It is therefore likely that the new drug candidates will have $V_{ss,\ ivt}$ in the range reported in Fig. 2B and del Amo et al. (2015). $V_{ss,\ ivt}$ values are similar or only moderately bigger than the anatomical volume of vitreal cavity and eye tissues, thereby ruling out the possibility that drug partitioning to the orbita would be significant. This is understandable, because the ocular blood flow removes drug effectively thereby minimizing its access to the orbita.

Drug elimination from the vitreous shows substantial differences among the compounds in the literature: CL_{ivt} values range from 0.011 to 1.530 ml/h (139-fold difference) and the values decrease clearly with increasing MW (Fig. 2A). Also, the $t_{1/2,\ ivt}$ values have a broad range (del Amo et al., 2015; Kidron et al., 2012), because the $t_{1/2,\ ivt}$ is dependent on CL_{ivt} and $V_{ss,\ ivt}$.

The CL_{ivt} of macromolecules are low (0.011–0.027 ml/h, Fig. 2A and D) because they are mainly eliminated via anterior route (Fig. 1A). Interestingly, CL_{ivt} of macromolecules are clearly less than

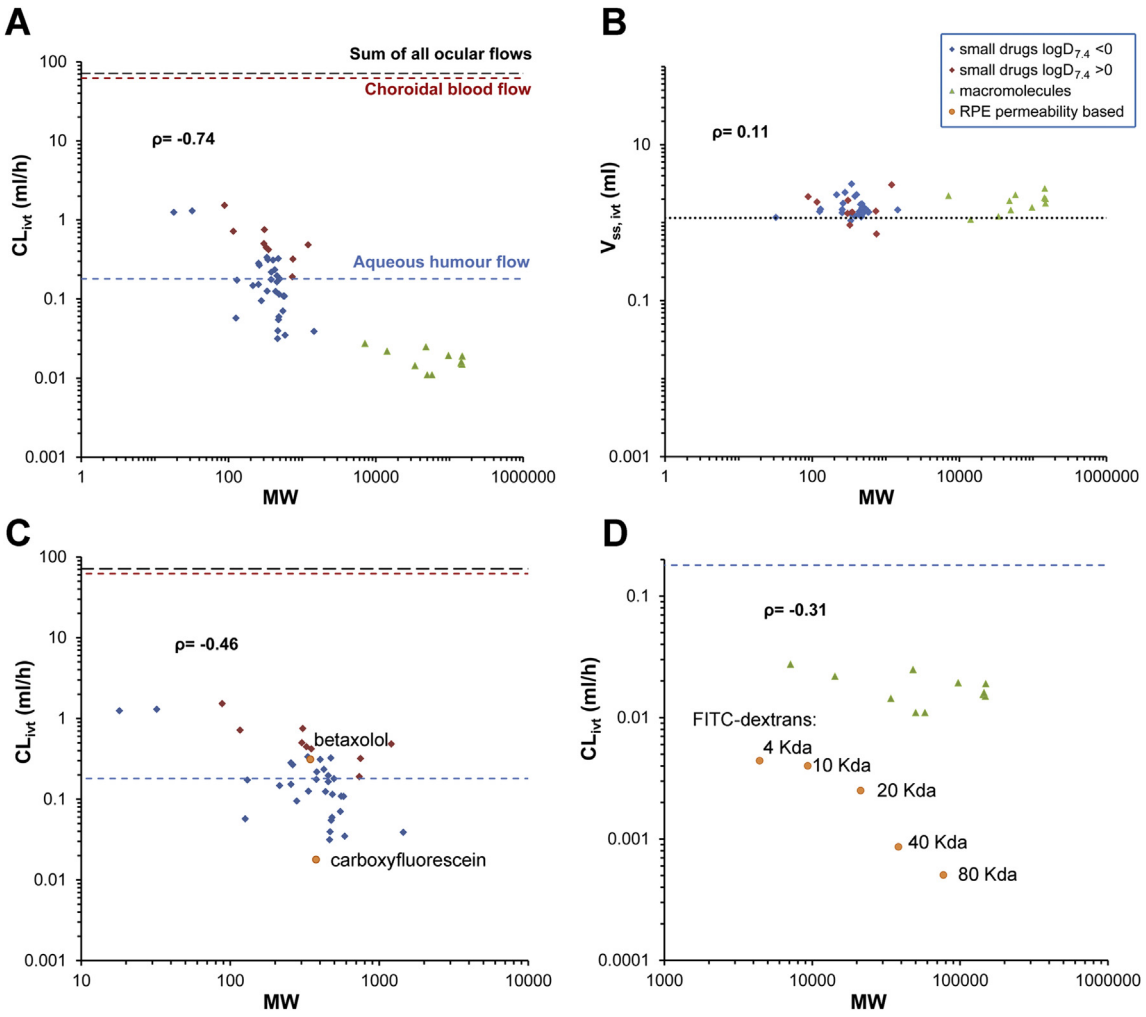

Fig. 2. The relationships between (A) MW and CL_{ivt} and (B) MW and $V_{ss,\ ivt}$ are presented for 40 small molecular compounds and 11 macromolecules after intravitreal injections in rabbits. The relationships between MW and CL_{ivt} of the small molecular compounds (C) and macromolecules (D) are presented. The diamonds represent the small MW compounds with Log $D_{7.4}$ below 0 (blue symbols) and Log $D_{7.4}$ above 0 (red symbols). The triangles represent the macromolecules. The circles represents intravitreal clearance via permeation across the RPE. These values were calculated based on permeability in bovine RPE-choroid membrane (Mannermaa et al., 2010; Pitkanen et al., 2005) and RPE surface area in rabbit (Reichenbach et al., 1994) using Eq. (4). In (A) the long dashed black line represents the sum of the ocular flow factors (choroidal, retinal, iridial and ciliary body blood flows, and aqueous humor flow), the short dashed lines correspond to the choroidal blood flow (red) and aqueous humor flow (blue). In (B) the dotted line represents the anatomical volume of the vitreous 1.15 ml. The ρ represent Spearman's rank correlation coefficient for small drugs and macromolecules. In the original publication (del Amo et al., 2015), the pharmacokinetic parameters of PF-04523655 were extracted from an abstract (Johnson, 2010). The original concentration curve became recently available and it was analyzed. However, the initial concentrations were too low for the administered dose. Therefore, the parameters of this drug were omitted from the figures.

the rate of aqueous humor turnover (0.18 ml/h) (Barany and Kinsey, 1949) suggesting that the access of drug from the vitreous to the anterior chamber is restricted. Presumably, CL_{ivt} of macromolecules via posterior route through blood-retina barrier is low, due to their low permeability in the RPE (Pitkanen et al., 2005). Intravitreal clearance across the RPE (CL_{RPE}) was calculated using the bovine RPE permeability for FITC-dextrans (Pitkanen et al., 2005) and surface area of the rabbit RPE (5.2 cm^2) (Reichenbach et al., 1994) according to Eq. (4) ($P \times S$). These CL_{RPE} values are 5–30 times lower than the CL_{ivt} values for the macromolecules in the same MW range (Fig. 2D). This suggests that only a small fraction (3–20%) of the macromolecule dose is eliminated through the RPE.

The wide range of CL_{ivt} of small drugs (0.031–1.530 ml/h) is probably determined by their ability to cross the blood-ocular barriers. High permeability across the barriers should lead to high CL_{ivt} values. Owing to the large surface area of the RPE and high blood flow in the choroid, it is probable that the compounds with high CL_{ivt} values are eliminated via posterior route (Fig. 1B). In our previous studies, the $t_{1/2,\ ivt}$ and CL_{ivt} of small drugs were determined by H-bond capacity and $LogD_{7.4}$ (del Amo et al., 2015; Kidron et al., 2012). These descriptors typically define membrane permeability, e.g. in the cornea (Kidron et al., 2010), intestinal wall (Linnankoski et al., 2006) and blood–brain barrier (Lanevskij et al., 2009; Liu et al., 2004). Accordingly, the calculated CL_{RPE} values for betaxolol and carboxyfluorescein, using permeability values of Pitkanen et al. (2005) and Mannermaa et al. (2010), are in the same range with CL_{ivt} values of lipophilic and hydrophilic small molecules, respectively, suggesting significant elimination through the RPE (Fig. 2C). Despite their ability to cross blood-retina barrier, the CL_{ivt} values of the small molecules are far below the value of choroidal blood flow showing that clearance is permeability-limited and not controlled by blood flow (Fig. 2A).

Some clinical biologics (e.g. ranibizumab, bevacizumab) are delivered intravitreally to the retinal and choroidal tissues. We should note that the effects of these drugs are dependent on their target concentrations and not on the quantity of drug that is eliminated through the blood-retina barrier. Therefore, therapeutic effects in the retina and/or choroid do not mean that the

posterior elimination pathway would be significant route for macromolecules. Therapeutic concentrations can be reached in the retina and/or choroid even though the posterior clearance would be an order of magnitude less than the anterior elimination.

3. Intravitreal pharmacokinetics in human eye

Intravitreal pharmacokinetic studies in humans are sparse, because the vitreous sampling is invasive and potentially risky procedure. There are, however, some studies that were carried out in patients who were selected for vitrectomy surgery or undergoing treatments for endophthalmitis, cytomegalovirus retinitis or choroidal neovascularization (Table 3). Typically, these studies reported only a few drug concentrations, usually from one individual and during the terminal elimination phase of the drug. For such data it is not possible to calculate the CL_{ivt} as it has been presented in Section 2.3. However, we did the following exercise to get rough estimates of CL_{ivt} (apparent CL_{ivt}), assuming one-compartment pharmacokinetics:

$$apparent\ CL_{ivt} = \frac{D_{ivt}}{AUC} \quad (6)$$

where D_{ivt} is the given intravitreal dose and AUC is area under the curve. The AUC values were calculated using equation (7):

$$AUC = \frac{C_0}{k_{elimination}} \quad (7)$$

where C_0 is the drug concentration in vitreous at time zero and $k_{elimination}$ is the first-order elimination rate constant. C_0 was calculated with equation (8):

$$C_0 = \frac{D_{ivt}}{V_{ss,\ ivt}} \quad (8)$$

where $V_{ss,\ ivt}$ was assumed to be equal to the human vitreous volume of 4 ml (Ruby et al., 2006). This is probably a reliable estimate, because the rabbit $V_{ss,\ ivt}$ values are limited in a narrow range (80% of the values in the dataset of 51 compounds were between 1.18 and 2.28 ml) (del Amo et al., 2015) and close to the anatomical volume of the vitreous. The $k_{elimination}$ was the slope of the curve defined by the calculated C_0 and the experimental concentration values. The apparent CL_{ivt} values are presented in Table 3. The same calculations for 2-fold higher $V_{ss,\ ivt}$ value (8 ml) were carried out and presented in Fig. A1 (versus rabbit CL_{ivt}) and A.2 (versus MW) in appendices. Estimation of CL_{ivt} and apparent CL_{ivt} values in human eyes enables universal rabbit-to-human comparison of intravitreal drug elimination (Fig. 3). Drug clearance in rabbit and human vitreous correlated well ($\rho = 0.91$; Rabbit $CL_{ivt} = 1.41 \times$ Human apparent $CL_{ivt} + 0.04$, units are ml/h; $R^2 = 0.82$) and absolute differences of the clearance values are in within 3-fold range (13/15

Table 3
Intravitreal drug concentrations in vitreous after intravitreal injection of drugs in humans. In the first panel, pharmacokinetic parameters are calculated by compartmental model (section 2.3, Doc. A) and in the second panel, the apparent CL_{ivt} is calculated according to the description given in section 3.

Drugs	Dose (μg)	Subjects	Time (h)	C (μg/ml)	$V_{ss,\ ivt}$ (ml)	CL_{ivt} (ml/h)	$t_{1/2,\ ivt}$ (h)	References
Bevacizumab	1250	Patients with choroidal neovascularization	24	92.70	3.17	0.025	160.8	(Zhu et al. 2008)
			48	165.00	9.39	0.042	154.4	Own calculations
			72	84.80				
			96	48.70				
			264	22.90				
			408	0.33				
			1032	1.39				
			1296	0.39				
			1776	0.022				
			2280	0.005				
			2424	0.003				

Drugs	Dose (μg)	Subjects	Time (h)	C (μg/ml)	Apparent CL_{ivt} (ml/h)	References
Bevacizumab	1250	Patients with choroidal neovascularization	48	166.0[a]	0.036	(Beer et al. 2006)
			696	0.5[b]		
Bevacizumab	1250	Patients with diabetic retinopathy	672	0.107	0.028	(Moisseiev et al. 2014)
			1344	0.019		
Cidofovir	20	AIDS patient with cytomegalovirus retinitis	24	0.673	0.336	(Taskintuna et al. 1998)
Dexamethasone phosphate	383[d]	Patients with postoperative endophthalmitis with and without core vitrectomy	66	0.023	0.472	(Gan et al. 2005)
			69	0.027		
			70	0.040		
			71	0.018		
			71	0.014		
			72	0.036		
Fomivirsen	165	Patients with cytomegalovirus retinitis	1	39.24[c]	0.068	(Bejanian et al. 1999)
			72	10.61		
			168	0.39		
			168	0.78		
			336	0.26		
Foscarnet	504[d]	AIDS patient with cytomegalovirus retinitis	23.25	51.53	0.152	(Diaz-Llopis et al. 1992)
Ganciclovir	200	AIDS patient with cytomegalovirus retinitis	51.4	1.17	0.292	(Henry et al. 1987)
Ganciclovir	2000	Patients with cytomegalovirus retinitis	24	212.0	0.172	(Morlet et al. 1996)
			24	165.4		
			24	138.2		
			24	102.2		
			24	152.8		

(continued on next page)

Table 3 (*continued*)

Drugs	Dose (μg)	Subjects	Time (h)	C (μg/ml)	Apparent CL_{ivt} (ml/h)	References
			24	92.2		
			72	59.8		
			72	10.0		
			72	20.8		
			72	19.4		
			72	6.8		
			72	23.4		
Gentamicin	50	Patients with postoperative endophthalmitis with and without core vitrectomy	63	0.90	0.092	(Gan et al. 2001)
			66	1.41		
			69	3.30		
			69	1.21		
			69	1.01		
			71	1.91		
			71	1.40		
			71	1.80		
			72	1.40		
			72	2.41		
			72	1.01		
			90	1.21		
			92	2.61		
Vancomycin	975[d]	Patients with postoperative endophthalmitis with core or entire vitrectomy	44	58.11	0.068	(Ferencz et al. 1999)
			48	137.85		
			72	182.36		
			72	25.05		
Vancomycin	200	Patients with postoperative endophthalmitis with and without core vitrectomy	63	2.59	0.084	(Gan et al. 2001)
			66	12.07		
			68	10.75		
			69	18.03		
			69	8.23		
			69	11.97		
			71	15.54		
			71	6.30		
			71	9.02		
			71	13.28		
			72	8.89		
			72	10.10		
			72	6.85		
			90	5.80		
			90	3.05		
			92	16.59		
			93	4.59		
Vancomycin	1000	Patients with postoperative endophthalmitis	48	125	0.100	(Haider et al. 2001)
			48	164		
			72	21		
			72	83		
Vancomycin	2000	Patients with postoperative endophthalmitis	48	161	0.100	(Haider et al. 2001)
			72	56		
			72	220		
			72	105		
			72	39		
Vancomycin	975[d]	Patients with exogenous endophthalmitis with core vitrectomy	24	133.7	0.132	(Raju et al. 2004)
			24	179.0		
			24	171.1		
			48	72.5		
			48	43.9		
Vancomycin	200	Patients with postoperative endophthalmitis with and without core vitrectomy	62	2.6	0.092	(Gan et al. 2005)
			66	12.0		
			68	10.8		
			69	12.0		
			69	8.2		
			71	15.5		
			71	9.0		
			71	8.9		
			71	6.3		
			71	16.6		
			72	6.8		
			93	4.6		

Footnote.

[a] The patient developed endophthalmitis 2 days after the drug injection, complete drug washout of previous treatment is assumed.

[b] The patient suffered retinal detachment 8 days before vitreous sampling.

[c] Average concentration of five patients. All other reported concentrations correspond to individual patient samples and only in Morlet's study (Morlet et al. 1996) two vitreous samples were taken from the same patient, for four patients.

[d] Equivalent dose.

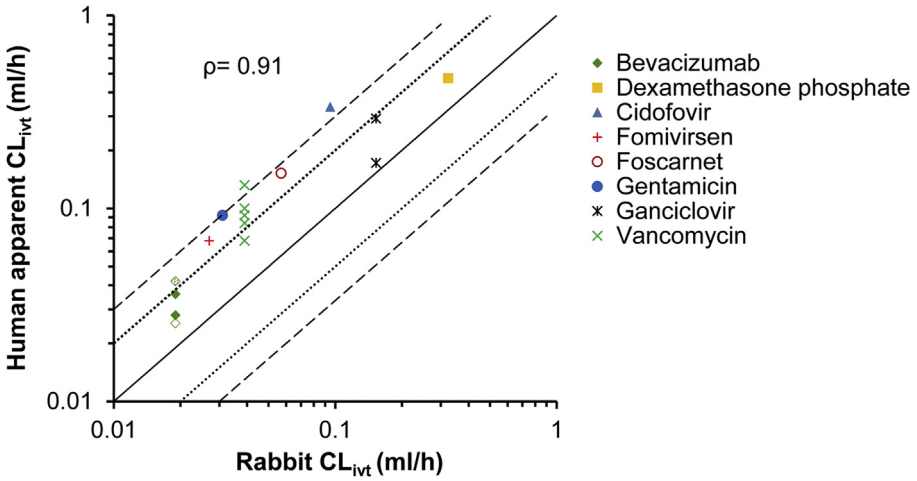

Fig. 3. Correlation between CL_{ivt} in rabbit versus human apparent CL_{ivt} (and CL_{ivt}). The dotted and dashed lines represent 2- and 3-fold deviation and the solid line represents the slope of 1.0. The open diamond correspond to bevacizumab CL_{ivt} calculated by Zhu et al. and the dotted one correspond to our calculations.

studies). The relationship of the apparent CL_{ivt} in human eye and MW was negative (Fig. B in appendices), like in rabbits (Fig. 2A). If higher value is used for human $V_{ss,\ ivt}$ (8 ml), the trends remain the same, and the CL_{ivt} difference is within 4-fold range (12/15 studies) (Fig. A1 and A2 in appendices). It is important to note that the individual values of apparent CL_{ivt} in human vitreous may not be accurate descriptors for the elimination of individual drugs. However, Fig. 3 shows good correlation and only moderate inter-species CL_{ivt} differences in the large pooled data from 15 studies. This supports the use of rabbit as a model in intravitreal pharmacokinetic studies. It is important to note that the human patients had different disease conditions (Table 3), but still no striking outliers were seen in the rabbit-to-man correlation in Fig. 3.

The experiment of Zhu et al. (2008) is the only human study that allows calculation of CL_{ivt} values with curve fitting (Table 3) though only one sample was available for each time point. It is important to note that bevacizumab has similar CL_{ivt} values (1.5- and 2.1-fold differences) in rabbit and humans (Fig. 3, Doc. A).

Intravitreal pharmacokinetics in human eyes is evaluated also by monitoring drug concentrations in the aqueous humor. Major concentration differences of bevacizumab in aqueous humor were seen after intravitreal injections in human (Krohne et al., 2008) and rabbit eyes (Nomoto et al., 2009). Based on this argument, the rabbit was considered not to be a good animal model for human eye (Rowe-Rendleman et al., 2014). However, that particular rabbit study (Nomoto et al., 2009) has some quality concerns: the first sample was taken only one week after the intravitreal injection and the assayed samples had exceptionally low concentrations. The authors compared their results with the rabbit study of Bakri et al. (Bakri et al., 2007) and justified the concentration differences based on the analytical method used. Nomoto et al. (2009) measured all variants of bevacizumab (free, in complex, fragments), but this kind of non-specific assay should lead to higher concentration values, not lower, than in Bakri's study. Then, it is interesting to plot together the existing rabbit and human data. The human bevacizumab data (Krohne et al., 2008; Meyer et al., 2011) is in line with Bakri's levels of bevacizumab in aqueous humor (Fig. 4). Similar conclusion is reached when AUC values of bevacizumab (normalized to 1 mg intravitreal dose) in aqueous humor are compared (Table 4): Nomoto's study (Nomoto et al., 2009) is clearly an outlier. Unfortunately, much criticism against rabbit model has been based on the comparisons of human data with Nomoto's rabbit data.

We carried out pharmacokinetic simulations of intravitreal bevacizumab using the measured pharmacokinetic parameters from the literature. We assumed that bevacizumab distributes in the vitreous as indicated by the $V_{ss,\ ivt}$ values (human 9.39 ml, rabbit 2.02 ml), its elimination takes place only via anterior route (CL_{ivt} = human 0.042 ml/h, rabbit 0.019 ml/h), and the elimination from the aqueous humor (volume 0.3 ml) takes place at the rate of aqueous humor outflow (human 0.14 ml/h, rabbit 0.18 ml/h) (Fig. 5, Table 5). Since blood-aqueous barrier does not allow permeation of proteins, the aqueous humor flow remains as the only route of bevacizumab elimination (Maurice and Mishima, 1984). The results

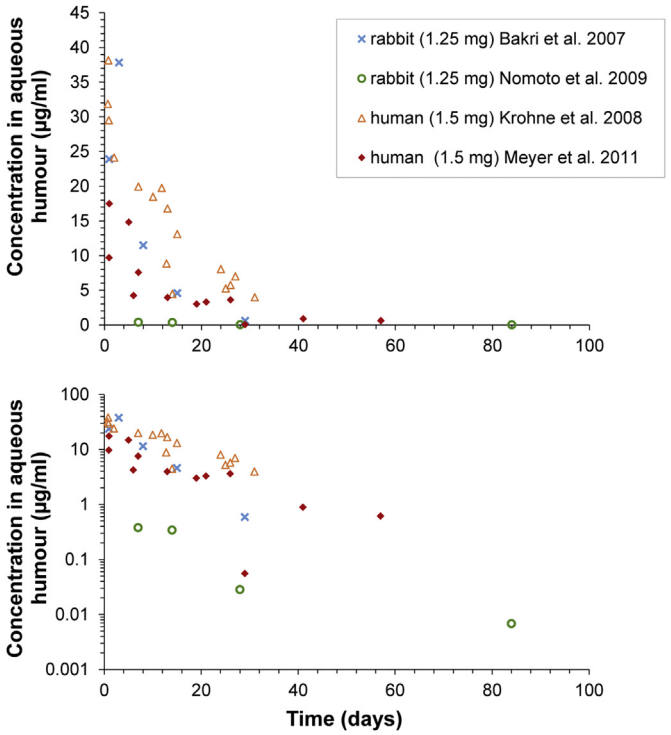

Fig. 4. Concentration of bevacizumab in aqueous humor versus time after intravitreal injection in rabbit (Bakri et al., 2007; Nomoto et al., 2009) and in human eyes (Krohne et al., 2008; Meyer et al., 2011) in arithmetic and semi-logarithmic scale.

Table 4
The AUC values (0 – infinity) of bevacizumab in aqueous humor after intravitreal injection in rabbit and human. The AUC values were dose normalized to 1 mg dose.

		AUC (μg*days)/ml	$AUC_{simulated}$ (μg*days)/ml
Rabbit	Bakri et al., 2007	234.6	231.5
	Nomoto et al., 2009	7.1	
Human	Krohne et al., 2008	325.2	297.3
	Meyer et al., 2011	131.8	

and structure of the simulation model are shown in Fig. 5. The simulated bevacizumab concentrations are in line with the real values, except the data of Nomoto et al. (Nomoto et al., 2009) that deviates substantially from the simulations (Figs. 4 and 5). The same conclusion is reached when AUC values of the simulations are compared to the experimental values (Table 4).

It is important to note that the drug concentrations in the aqueous humor are different from the concentrations in the vitreous. Moreover, the ratio of the concentrations (aqueous humor/vitreous) may not be constant for all compounds. Based on simulation, $AUC_{aqueous\ humor}/AUC_{vitreous}$ for small lipophilic compound (CL_{ivt} = 0.5 ml/h, $CL_{aqueous\ humor}$ = 1.2 ml/h (Schoenwald, 2003)) is 0.016. This means that the drug concentrations in the vitreous are approximately 50 times greater than in the aqueous humor. In the case of bevacizumab, the AUC-ratio is 0.095 meaning that approximately 10-fold higher concentrations are seen in the vitreous than in the aqueous humor.

4. Role of the vitreous in intravitreal pharmacokinetics

Many studies suggest that the vitreous plays a role in ocular pharmacokinetics, because the clearance of small MW drugs is faster in vitrectomized and lensectomized rabbit eyes than in either lensectomized or control rabbit eyes (Doft et al., 1985; Ficker et al., 1990; Jarus et al., 1985; Mandell et al., 1993; Pearson et al., 1993; Pflugfelder et al., 1987; Wingard et al., 1989). However, there are many changing variables in such studies (Doft et al., 1985; Ficker et al., 1990; Mandell et al., 1993; Wingard et al., 1989), and it is impossible to distinguish the specific effects of vitreous from the experiments with vitrectomized and lensectomized eyes (Jarus et al., 1985; Pearson et al., 1993; Pflugfelder et al., 1987). There are a few studies with vitrectomized rabbit eyes without lensectomy (Ahn et al., 2013, 2014; Christoforidis et al., 2013; Lee et al., 2010). In vitrectomized rabbit eyes, pharmacokinetics of bevacizumab and ranibizumab did not differ from the control rabbits (Ahn et al., 2013, 2014), while in another study small (1.8- and 1.3-fold) differences were seen for bevacizumab and ranibizumab, respectively (Christoforidis et al., 2013). Likewise, small increase in the elimination of FITC-dextrans was shown in the rabbit eyes after hyaluronidase treatment (Tan et al., 2011). We must be cautious in the interpretations because vitrectomy or enzyme treatment may endanger the integrity of the blood-ocular barriers (Knudsen et al., 2001; Mochizuki et al., 1992, 1993).

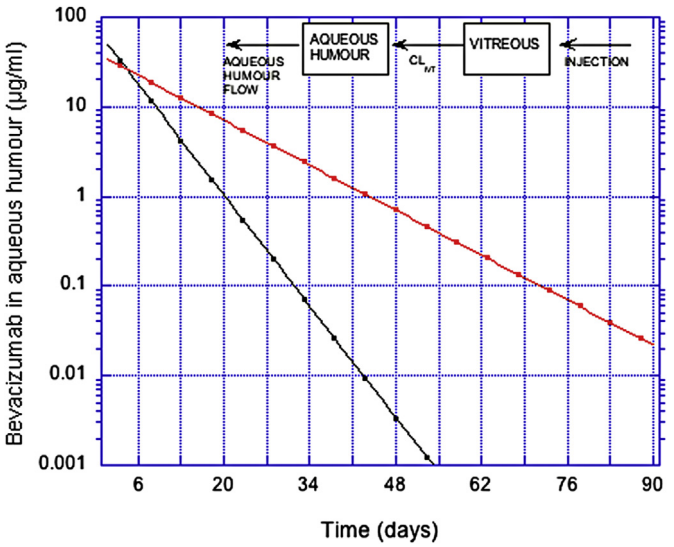

Fig. 5. The model structure and simulated bevacizumab concentrations in the human (in red) and rabbit (in black) aqueous humor are presented. The doses are as described in Fig. 3. (For interpretation of the references to color in this figure legend, the reader is referred to the web version of this article.)

Lee et al. (Lee et al., 2010) claimed a 10 times shorter $t_{1/2,\ ivt}$ for the vitrectomized rabbit as compared to the control rabbit. However, this study is misleading and data analysis is not reliable. In the operated eye, the half-life was calculated based on two experimental early data points, while additional later time point was included in the data analysis of the control eye. Moreover, the calculated $t_{1/2,\ ivt}$ in the control group was abnormally short considering that VEGF is a macromolecule. This problem has also been pointed out in other publications (Ahn et al., 2013, 2014). In conclusion, the study of Lee et al. (Lee et al., 2010) is an outlier among the studies on the vitreous effects on ocular pharmacokinetics. Most data does not support significant role of vitreous in drug elimination from the vitreous cavity.

Relatively minor effects of vitreous on ocular pharmacokinetics is understandable, because the vitreous is relatively loose structure that allows rapid diffusion of small molecular drugs and proteins (Gajraj, 2012; Maurice and Mishima, 1984; Pitkanen et al., 2003; Xu et al., 2000). Recently the mean pore size of the vitreous was analyzed to be 550 ± 50 nm, value that is two orders of magnitude greater than typical molecular diameter of a protein drug (Xu et al., 2013). Therefore, changes in the vitreous viscosity are not expected to have effects on drug diffusion and drug elimination from the eye. For example, diffusivity in the porcine and rabbit vitreous was similar (Gajraj, 2012) even though these species have difference in the viscosity of the vitreous. Furthermore, CL_{ivt} values show 139-fold range *in vivo* in rabbits (Fig. 2A). Compared to that range, the differences in the drug diffusion in the vitreous are negligible (Gajraj, 2012; Missel, 2012; Xu et al., 2000). Importantly, molecular permeability in the isolated RPE-choroid had 618-fold range of values depending on the lipophilicity and size of the compound (Pitkanen et al., 2005). Overall, permeability in the blood-retina barrier defines the range of CL_{ivt} values of drugs after intravitreal injections. In the case of small molecules, there is no correlation between MW and CL_{ivt} (Fig. 2C), but QSPR model with hydrogen bonding and $LogD_{7.4}$ describes the CL_{ivt} reliably (del Amo et al., 2015) showing clear dependence on blood-ocular barrier permeation.

For macromolecules the range of CL_{ivt} values is only about 3-fold, even though the MW range is 7122–149,000 (Fig. 2D). The CL_{RPE} values are much smaller than CL_{ivt} values indicating dominating role of the anterior elimination route, but yet CL_{ivt} values are clearly smaller than the rate of aqueous humor turnover (Fig. 2D). This is mainly due the restricted access of the drug from vitreous to the

Table 5
Comparison between the pharmacokinetically relevant anatomical and physiological parameters in the rabbit and human (or monkey) eye. The factors affecting the CL_{ivt} of macromolecules are marked by a dotted box. All parameters may affect the CL_{ivt} of small molecular drugs.

				Rabbit	*Human*	*References*
Physiological values affecting CL_{ivt}	Blood flow mediated CL_{ivt}	Barrier surface area	**Surface area of RPE**	520[a] mm^2	1204 ± 184[b] mm^2	(Reichenbach et al. 1994) (Panda-Jonas et al. 1994)
		Barrier permeability	**TEER of RPE layer**	179.2 ± 6 ohm.cm^2	79 ± 48 ohm.cm^2	(Koyano et al. 1993) (Quinn and Miller. 1992)
		Blood flows:	**Choroidal blood flow**	62 ml/h	43 ml/h	(Nilsson and Alm. 2012) (Sebag et al. 1994)
			Retinal blood flow	0.66 ml/h	0.26 ml/h	(Nilsson and Alm. 2012) (Feke et al. 1989)
			Ciliary body blood flow	4.91 ml/h	5.34[c] ml/h	(Nilsson and Alm. 2012) (Alm and Bill. 1973)
			Iridial blood flow	3.72 ml/h	1.02[c] ml/h	(Nilsson and Alm. 2012) (Alm and Bill. 1973)
	Aqueous humor flow mediated CL_{ivt}	Aqueous humor flow		0.18 ml/h	0.14 ml/h	(Barany and Kinsey. 1949) (Brubaker. 1982)
		Barrier between vitreous and anterior chamber		undefined	undefined	
Physiological values affecting $V_{ss,\ ivt}$ of all drugs		Ocular volumes:	**Vitreous volume**	1.15 ml	4 ml	(del Amo et al. 2015) (Ruby et al. 2006)
			Lens weight	0.33 - 0.53 g	0.15 - 0.26 g	(Zamudio and Candia. 2011) (Hemenger et al. 1995)
			Uveal tract & retina weight	0.16 g		(Wiederholt et al. 1986)
			Choroid weight	0.059 g		(Wu et al. 1970)
			Iris weight	0.057 g		(Wu et al. 1970)
			Ciliary body weight	0.050 g		(Wu et al. 1970)
		Tissue affinities:	$K_{p,\ ocular\ tissues}$	No data	No data	

Footnote: a: from adult rabbit; b: from humans between 2 and 90 year-old (50.7 ± 20.4 years); c: data from monkey, no human data available to our knowledge.

aqueous humor (i.e. bottleneck of the lens, ciliary body and lens) and partly due to the diffusion in the vitreous. Even though CL_{ivt} values of macromolecules may partly depend on their diffusivity in the vitreous, the values are spanning only a narrow range despite the large differences in the MWs. This is not surprising, because the pore size of non-liquefied vitreous (550 nm) is far greater than the size of protein drugs (about 5–10 nm) (Xu et al., 2013). Interestingly, CL_{ivt} values do not correlate with MW (Fig. 2D). This suggests that the role of vitreous may be related to the vitreous–proteins interactions, and not size related sieving effects.

Vitreous may have more significant effects on intravitreal pharmacokinetics in special cases. For example, highly cationic macromolecules, cationic nanoparticles and larger suspension particles show limited mobility and possible aggregation in the vitreous (Chin et al., 2005; Doft et al., 1985; Pitkanen et al., 2003; Wingard et al., 1989; Xu et al., 2013). These formulation aspects are, however, beyond the scope of this article.

5. Rabbit as an animal model in intravitreal pharmacokinetics

Successful translation of intravitreal pharmacokinetics from rabbit to man requires quantitative understanding of intravitreal pharmacokinetics in both. Unfortunately, there are only sparse data on human intravitreal pharmacokinetics. As presented in Sections 2 and 3, we have pooled all available data to calculate the primary pharmacokinetic parameters for the rabbit and human eye. The outcome does not support the criticism of rabbit as an animal model. Rather, it indicates that in general rabbit is a decent model in the vitreal pharmacokinetics.

$V_{ss,\ ivt}$ values depend on the anatomical volumes of the vitreous and surrounding tissues, and drug partitioning to the tissues (Section 2.1). Like in the rabbits, the human $V_{ss,\ ivt}$ values are expected to be close to human vitreous volume (4 ml), since the adjacent tissues are very small compared to the vitreous volume. Indeed, for bevacizumab (Zhu et al., 2008) the $V_{ss,\ ivt}$ in human was calculated as 3.2 ml and 9.4 ml (Table 3). These values were 1.6-fold and 4.5-fold higher than the $V_{ss,\ ivt}$ in rabbit (2.0 ml) (Bakri et al., 2007; Christoforidis et al., 2013; del Amo et al., 2015), while the difference in the vitreous volumes is between 2- and 3-fold (Table 5). Recently, Krohne et al. (2015) did not find significant impact of axial length and lens status on the pharmacokinetics of intravitreal ranibizumab and bevacizumab. This supports the notion that the $V_{ss,\ ivt}$ is relatively constant, mostly governed by the volume of the vitreous. On the contrary, systemic volumes of drug distribution span approximately 200,000-fold range (Obach et al., 2008). In conclusion, $V_{ss,\ ivt}$ in humans can be estimated with good accuracy based on the rabbit data and size difference of human and rabbit eye.

CL_{ivt} for small lipophilic molecules takes place mostly via RPE and choroid (Maurice and Mishima, 1984). The choroidal blood flow values in the rabbit and human are quite similar being about 85% of the total ocular blood flow (Table 5). It is known that both CL_{ivt} and RPE permeability are strongly affected by lipophilicity indicator ($LogD_{7.4}$) of the drug (del Amo et al., 2015; Pitkanen et al., 2005). Indeed, CL_{ivt} via RPE should be the product of drug permeability in the RPE and surface area of the RPE (Section 2.1, Eq. (4)). The RPE permeability in rabbit and human should be similar due to their similar trans-epithelial electrical resistance (TEER) values (Table 5), while the area of RPE is two to three times higher than in the rabbit. Therefore, CL_{ivt} of small lipophilic compounds is expected to be two or three times higher in man than in rabbit. This trend was

observed in Fig. 3. Apparent CL_{ivt} in humans was on average 1.4 times greater than the CL_{ivt} in rabbits. Anyway, the values are relatively similar and the correlation is good ($\rho = 0.91$, $R^2 = 0.82$).

One criticism has been based on the differences between the vasculature of the rabbit retina and the human retina. Nevertheless, in rabbit and human the retinal and choroidal blood flows are similar (Table 5) and the vascular walls as well (tight junctions in the retina; leaky vessels in the choroid). However, some issues of concern are related to the potential impact of the disease state on leakiness of the blood–ocular barriers, especially the RPE. Since CL_{ivt} is clearly permeability limited, changes in the rate–limiting membranes are expected to modify pharmacokinetics. This factor did not become evident in the data analysis based on the patients in Fig. 3, but we cannot exclude the possibility that some disease states might have significant impact on the intravitreal pharmacokinetics.

For macromolecules, anterior elimination via aqueous humor turnover is the main route of elimination. The rates of the aqueous humor turnover are similar in human and rabbit (Table 5), but these values are higher than the CL_{ivt} of macromolecules (Dejneka et al., 2008; del Amo et al., 2015; Eyetech Study Group, 2002; Leeds et al., 1997). Therefore, the access of the drug to the aqueous humor may limit its elimination in both rabbit and human eye. The CL_{ivt} values of bevacizumab in humans are 0.025 ml/h and 0.042 ml/h (Table 4), while in rabbit it is 0.019 ml/h (Bakri et al., 2007; Christoforidis et al., 2013; del Amo et al., 2015). The role of the barrier between vitreous and anterior chamber (lens, vitreous, zonules) remains unknown, but the data do not support major differences between man and rabbit.

In humans, the vitreous becomes more liquefied and less homogenous with the age, and this is associated with increased convective flow in the vitreal cavity (Maurice, 2001; Missel, 2012). Liquefaction and convection has been stated to be major pharmacokinetic differences between the rabbit and elderly patients (Laude et al., 2010). However, no significant difference in the intravitreal concentrations in patients with and without vitrectomy was observed in Gan's study (Gan et al., 2005) and the apparent CL_{ivt} value of vancomycin was not higher in vitrectomized patients (Ferencz et al., 1999) compared to non-vitrectomized patients (Haider et al., 2001) (Fig. 3, Table 2). Moreover, apparent CL_{ivt} values in elderly patients with and without vitrectomy were only moderately different from the CL_{ivt} values in healthy rabbits (Fig. 3, Table 2). Furthermore, Los (2008) showed that aging rabbit eye may be a good model for human vitreous liquefaction based on anatomical and histological analysis. Such a model may be a better approach than enzyme treatments to investigate the effect of the liquefying matrix or vitrectomy on vitreal drug elimination. Overall, even though vitreous humor may play a partial role in the elimination of macromolecules from the vitreal cavity, there is no evidence that the differences in the vitreal liquefaction or convection would cause significant changes in intravitreal pharmacokinetics (Fig. 3).

Drug metabolism in the liver is different in various species and, therefore, test methods based on human cells are being developed (Vellonen et al., 2014). The metabolic activity in the eye is relatively small if any. In general, intravitreal drugs are eliminated from the eye via elimination across the blood-ocular barriers and aqueous humor outflow, and not via metabolism (del Amo et al., 2015). Comparison between the rabbit and human data has not revealed metabolism derived species differences in vitreal drug elimination.

Even though the eye is partly immune protected site, there is a possibility that intravitreal injection of human protein or humanized antibody could cause immune response in the eye. Impact of immune response on intravitreal pharmacokinetics has not been demonstrated, even though Gaudreault et al. (2007) discussed this possibility. Formation of anti-drug antibodies can have substantial influence on systemic clearance of some protein-based drugs (Chen et al., 2013). The neutralizing antibodies are formed in a few weeks. Therefore, the immunological influence on intravitreal pharmacokinetics is expected to be minimal after a single injection, but may become evident during multiple dosing therapy.

Sometimes binding of drug to target proteins determines the drug clearance from the systemic circulation (Levy, 1994). For example, FcRN receptors mediate clearance of monoclonal antibodies from the systemic circulation so that the receptor turnover processes bring drug back to the blood circulation thereby prolonging the retention in the circulation (Ezan, 2013; Mager and Jusko, 2001). This leads sometimes also to receptor saturation and dose-dependent clearance, i.e. increasing clearance at higher doses. In principle, such mechanisms might operate within the eye, but so far they have not been shown to exist.

This review has concentrated on intravitreal pharmacokinetics of drugs in solution form. There is an increasing interest on ocular drug delivery systems for prolonged and controlled drug delivery to the posterior eye segment (del Amo and Urtti, 2008). The functionality of the dosage forms in the rabbit and human eye is beyond the scope of this review. Anyway, CL_{ivt} values are useful in the design of drug delivery systems, because the required release rate *in vivo* depends on the target concentration and CL_{ivt} (del Amo et al., 2015). Furthermore, the required drug payload in the dosage form is release rate multiplied by the dosing interval. As only small volumes can be injected intravitreally (maximum 100 μl), computational estimation of drug payload is very important aid in the design of prolonged action dosage forms for the retinal treatment. Overall, CL_{ivt} should be taken into account in the design of new intravitreal drug delivery systems.

6. Conclusions

In this review we have analyzed the data on intravitreal pharmacokinetics in rabbits and humans. Overall, based on the current data the rabbit is clinically predictable animal model for intravitreal pharmacokinetics, since both intravitreal volume of distribution and clearance values differ only moderately between rabbit and human. Intravitreal pharmacokinetic studies should be designed so that accurate values for clearance and volume of distribution are obtained. Further studies are needed in special cases, such as disease state effects, to complement the understanding of intravitreal pharmacokinetics.

Acknowledgments

This study was supported by the Finnish Cultural Foundation (E.d.A.) and Academy of Finland (A.U., project number 268868).

Appendix A. Supplementary data

Supplementary data related to this article can be found at http://dx.doi.org/10.1016/j.exer.2015.05.003.

References

Ahn, J., Kim, H., Woo, S.J., Park, J.H., Park, S., Hwang, D.J., Park, K.H., 2013. Pharmacokinetics of intravitreally injected bevacizumab in vitrectomized eyes. J. Ocul. Pharmacol. Ther. 29, 612–618.

Ahn, S.J., Ahn, J., Park, S., Kim, H., Hwang, D.J., Park, J.H., Park, J.Y., Chung, J.Y., Park, K.H., Woo, S.J., 2014. Intraocular pharmacokinetics of ranibizumab in vitrectomized versus nonvitrectomized eyes. Invest. Ophthalmol. Vis. Sci. 55, 567–573.

Alm, A., Bill, A., 1973. Ocular and optic nerve blood flow at normal and increased intraocular pressures in monkeys (Macaca irus): a study with radioactively labelled microspheres including flow determinations in brain and some other

tissues. Exp. Eye Res. 15, 15–29.
Atluri, H., Mitra, A.K., 2003. Disposition of short-chain aliphatic alcohols in rabbit vitreous by ocular microdialysis. Exp. Eye Res. 76, 315–320.
Bakri, S.J., Snyder, M.R., Reid, J.M., Pulido, J.S., Singh, R.J., 2007. Pharmacokinetics of intravitreal bevacizumab (Avastin). Ophthalmology 114, 855–859.
Barany, Y.E., Kinsey, V.E., 1949. The rate of flow of aqueous humor; the rate of disappearance of para-aminohippuric acid, radioactive rayopake, and radioactive diodrast from the aqueous humor of rabbits. Am. J. Ophthalmol 32, 177–188. Pt. 2.
Bashshur, Z.F., Haddad, Z.A., Schakal, A., Jaafar, R.F., Saab, M., Noureddin, B.N., 2008. Intravitreal bevacizumab for treatment of neovascular age-related macular degeneration: a one-year prospective study. Am. J. Ophthalmol. 145, 249–256 e2.
Beer, P.M., Wong, S.J., Hammad, A.M., Falk, N.S., O'Malley, M.R., Khan, S., 2006. Vitreous levels of unbound bevacizumab and unbound vascular endothelial growth factor in two patients. Retina 26, 871–876.
Bejanian, M., Lieberman, R.M., Goldstein, D.A., Engstrom, R.E., Boyer, D.S., Dunn, J.P., 1999. A pharmacokinetic study of intravitreal fomivirsen in patients with CMVR. Invest. Opthalmol. Vis. Sci. 40. S874–Abstract.
Brubaker, R.F., 1982. The flow of aqueous humor in the human eye. Trans. Am. Ophthalmol. Soc. 80, 391–474.
Cheung, L.K., Eaton, A., 2013. Age-related macular degeneration. Pharmacotherapy 33, 838–855.
Chen, X., Hickling, T., Kraynov, E., Kuang, B., Parng, C., Vicini, P., 2013. A mathematical model of the effect of immunogenicity on therapeutic protein pharmacokinetics. AAPS J. 15, 1141–1154.
Chin, H.S., Park, T.S., Moon, Y.S., Oh, J.H., 2005. Difference in clearance of intravitreal triamcinolone acetonide between vitrectomized and nonvitrectomized eyes. Retina 25, 556–560.
Christoforidis, J.B., Carlton, M.M., Knopp, M.V., Hinkle, G.H., 2011. PET/CT imaging of I-124-radiolabeled bevacizumab and ranibizumab after intravitreal injection in a rabbit model. Invest. Ophthalmol. Vis. Sci. 52, 5899–5903.
Christoforidis, J.B., Williams, M.M., Kothandaraman, S., Kumar, K., Epitropoulos, F.J., Knopp, M.V., 2012. Pharmacokinetic properties of intravitreal i-124-aflibercept in a rabbit model using PET/CT. Curr. Eye Res. 37, 1171–1174.
Christoforidis, J.B., Williams, M.M., Wang, J., Jiang, A., Pratt, C., Abdel-Rasoul, M., Hinkle, G.H., Knopp, M.V., 2013. Anatomic and pharmacokinetic properties of intravitreal bevacizumab and ranibizumab after vitrectomy and lensectomy. Retina 33, 946–952.
Dejneka, N.S., Wan, S., Bond, O.S., Kornbrust, D.J., Reich, S.J., 2008. Ocular biodistribution of bevasiranib following a single intravitreal injection to rabbit eyes. Mol. Vis. 14, 997–1005.
del Amo, E.M., Urtti, A., 2008. Current and future ophthalmic drug delivery systems. A shift to the posterior segment. Drug Discov. Today 13, 135–143.
del Amo, E.M., Vellonen, K., Kidron, H., Urtti, A., 2015. Intravitreal clearance and volume of distribution of compounds in rabbits: In silico prediction and pharmacokinetic simulations for drug development. Eur. J. Pharm. Biopharm. http://dx.doi.org/10.1016/j.ejpb.2015.01.003.
Diaz-Llopis, M., Chipont, E., Sanchez, S., Espana, E., Navea, A., Menezo, J.L., 1992. Intravitreal foscarnet for cytomegalovirus retinitis in a patient with acquired immunodeficiency syndrome. Am. J. Ophthalmol. 114, 742–747.
Doft, B.H., Weiskopf, J., Nilsson-Ehle, I., Wingard Jr., L.B., 1985. Amphotericin clearance in vitrectomized versus nonvitrectomized eyes. Ophthalmology 92, 1601–1605.
Durairaj, C., Kim, S.J., Edelhauser, H.F., Shah, J.C., Kompella, U.B., 2009. Influence of dosage form on the intravitreal pharmacokinetics of diclofenac. Invest. Ophthalmol. Vis. Sci. 50, 4887–4897.
Duvvuri, S., Gandhi, M.D., Mitra, A.K., 2003. Effect of P-glycoprotein on the ocular disposition of a model substrate, quinidine. Curr. Eye Res. 27, 345–353.
Eyetech Study Group, 2002. Preclinical and phase 1A clinical evaluation of an anti-VEGF pegylated aptamer (EYE001) for the treatment of exudative age-related macular degeneration. Retina 22, 143–152.
Ezan, E., 2013. Pharmacokinetic studies of protein drugs: past, present and future. Adv. Drug Deliv. Rev. 65, 1065–1073.
Feke, G.T., Tagawa, H., Deupree, D.M., Goger, D.G., Sebag, J., Weiter, J.J., 1989. Blood flow in the normal human retina. Invest. Ophthalmol. Vis. Sci. 30, 58–65.
Ferencz, J.R., Assia, E.I., Diamantstein, L., Rubinstein, E., 1999. Vancomycin concentration in the vitreous after intravenous and intravitreal administration for postoperative endophthalmitis. Arch. Ophthalmol. 117, 1023–1027.
Ficker, L., Meredith, T.A., Gardner, S., Wilson, L.A., 1990. Cefazolin levels after intravitreal injection. Effects of inflammation and surgery. Invest. Ophthalmol. Vis. Sci. 31, 502–505.
Gajraj, R.T.C., 2012. A Study of Drug Transport in the Vitreous Humor: Effect of Drug Size; Comparing Micro- and Macro-scale Diffusion; Assessing Vitreous Models; and Obtaining in Vivo Data. https://tspace.library.utoronto.ca/handle/1807/33202.
Gan, I.M., Ugahary, L.C., van Dissel, J.T., van Meurs, J.C., 2005. Effect of intravitreal dexamethasone on vitreous vancomycin concentrations in patients with suspected postoperative bacterial endophthalmitis. Graefes Arch. Clin. Exp. Ophthalmol. 243, 1186–1189.
Gan, I.M., van Dissel, J.T., Beekhuis, W.H., Swart, W., van Meurs, J.C., 2001. Intravitreal vancomycin and gentamicin concentrations in patients with postoperative endophthalmitis. Br. J. Ophthalmol. 85, 1289–1293.
Gaudreault, J., Fei, D., Beyer, J.C., Ryan, A., Rangell, L., Shiu, V., Damico, L.A., 2007. Pharmacokinetics and retinal distribution of ranibizumab, a humanized antibody fragment directed against VEGF-A, following intravitreal administration in rabbits. Retina 27, 1260–1266.
Gillette, J.R., 1971. Factors affecting drug metabolism. Ann. N. Y. Acad. Sci. 179, 43–66.
Gupta, S.K., Velpandian, T., Dhingra, N., Jaiswal, J., 2000. Intravitreal pharmacokinetics of plain and liposome-entrapped fluconazole in rabbit eyes. J. Ocul. Pharmacol. Ther. 16, 511–518.
Haider, S.A., Hassett, P., Bron, A.J., 2001. Intraocular vancomycin levels after intravitreal injection in post cataract extraction endophthalmitis. Retina 21, 210–213.
Hemenger, R.P., Garner, L.F., Ooi, C.S., 1995. Change with age of the refractive index gradient of the human ocular lens. Invest. Ophthalmol. Vis. Sci. 36, 703–707.
Henry, K., Cantrill, H., Fletcher, C., Chinnock, B.J., Balfour Jr., H.H., 1987. Use of intravitreal ganciclovir (dihydroxy propoxymethyl guanine) for cytomegalovirus retinitis in a patient with AIDS. Am. J. Ophthalmol. 103, 17–23.
Hughes, P.M., Krishnamoorthy, R., Mitra, A.K., 1996. Vitreous disposition of two acycloguanosine antivirals in the albino and pigmented rabbit models: a novel ocular microdialysis technique. J. Ocul. Pharmacol. Ther. 12, 209–224.
Iyer, M.N., He, F., Wensel, T.G., Mieler, W.F., Benz, M.S., Holz, E.R., 2006. Clearance of intravitreal moxifloxacin. Invest. Ophthalmol. Vis. Sci. 47, 317–319.
Jarus, G., Blumenkranz, M., Hernandez, E., Sossi, N., 1985. Clearance of intravitreal fluorouracil. Normal and aphakic vitrectomized eyes. Ophthalmology 92, 91–96.
Johnson, T.R., 2010. Pharmacokinetic and ocular distribution of PF-04523655 and RTP801-inhibiting siRNA, following intravitreal administration in rabbits. Invest. Ophthalmol. Vis. Sci. 51. E-Abstract 2442.
Jusko, W.J., 2006. Guidelines for collection and analysis for pharmacokinetic data. In: Burton, M.E. (Ed.), Applied Pharmacokinetics and Applied Therapeutics, fourth ed. Lippincott Williams & Wilkins, pp. 9–26.
Kidron, H., del Amo, E.M., Vellonen, K.S., Urtti, A., 2012. Prediction of the vitreal half-life of small molecular drug-like compounds. Pharm. Res. 29, 3302–3311.
Kidron, H., Vellonen, K.S., del Amo, E.M., Tissari, A., Urtti, A., 2010. Prediction of the corneal permeability of drug-like compounds. Pharm. Res. 27, 1398–1407.
Knudsen, L.L., Dissing, T., Hansen, M.N., Nielsen-Kudsk, F., 2001. Ocular fluorescein kinetics before and after vitrectomy on swine. Graefes Arch. Clin. Exp. Ophthalmol. 239, 832–839.
Kontturi, L.S., Collin, E.C., Murtomaki, L., Pandit, A.S., Yliperttula, M., Urtti, A., 2014. Encapsulated cells for long-term secretion of soluble VEGF receptor 1: material optimization and simulation of ocular drug response. Eur. J. Pharm. Biopharm. http://dx.doi.org/10.1016/j.ejpb.2014.10.005.
Koyano, S., Araie, M., Eguchi, S., 1993. Movement of fluorescein and its glucuronide across retinal pigment epithelium-choroid. Invest. Ophthalmol. Vis. Sci. 34, 531–538.
Krohne, T.U., Eter, N., Holz, F.G., Meyer, C.H., 2008. Intraocular pharmacokinetics of bevacizumab after a single intravitreal injection in humans. Am. J. Ophthalmol. 146, 508–512.
Krohne, T.U., Muether, P.S., Stratmann, N.K., Holz, F.G., Kirchhof, B., Meyer, C.H., Fauser, S., 2015. Influence of ocular volume and lens status on pharmacokinetics and duration of action of intravitreal vascular endothelial growth factor inhibitors. Retina 35, 69–74.
Lanevskij, K., Japertas, P., Didziapetris, R., Petrauskas, A., 2009. Ionization-specific prediction of blood-brain permeability. J. Pharm. Sci. 98, 122–134.
Laude, A., Tan, L.E., Wilson, C.G., Lascaratos, G., Elashry, M., Aslam, T., Patton, N., Dhillon, B., 2010. Intravitreal therapy for neovascular age-related macular degeneration and inter-individual variations in vitreous pharmacokinetics. Prog. Retin. Eye Res. 29, 466–475.
Lee, S.S., Ghosn, C., Yu, Z., Zacharias, L.C., Kao, H., Lanni, C., Abdelfattah, N., Kuppermann, B., Csaky, K.G., D'Argenio, D.Z., Burke, J.A., Hughes, P.M., Robinson, M.R., 2010. Vitreous VEGF clearance is increased after vitrectomy. Invest. Ophthalmol. Vis. Sci. 51, 2135–2138.
Leeds, J.M., Henry, S.P., Truong, L., Zutshi, A., Levin, A.A., Kornbrust, D., 1997. Pharmacokinetics of a potential human cytomegalovirus therapeutic, a phosphorothioate oligonucleotide, after intravitreal injection in the rabbit. Drug Metab. Dispos. 25, 921–926.
Levy, G., 1994. Pharmacologic target-mediated drug disposition. Clin. Pharmacol. Ther. 56, 248–252.
Linnankoski, J., Makela, J.M., Ranta, V.P., Urtti, A., Yliperttula, M., 2006. Computational prediction of oral drug absorption based on absorption rate constants in humans. J. Med. Chem. 49, 3674–3681.
Liu, X., Tu, M., Kelly, R.S., Chen, C., Smith, B.J., 2004. Development of a computational approach to predict blood-brain barrier permeability. Drug Metab. Dispos. 32, 132–139.
Los, L.I., 2008. The rabbit as an animal model for post-natal vitreous matrix differentiation and degeneration. Eye (Lond) 22, 1223–1232.
Mager, D.E., 2006. Quantitative structure-pharmacokinetic/pharmacodynamic relationships. Adv. Drug Deliv. Rev. 58, 1326–1356.
Mager, D.E., Jusko, W.J., 2001. General pharmacokinetic model for drugs exhibiting target-mediated drug disposition. J. Pharmacokinet. Pharmacodyn. 28, 507–532.
Mandell, B.A., Meredith, T.A., Aguilar, E., el-Massry, A., Sawant, A., Gardner, S., 1993. Effects of inflammation and surgery on amikacin levels in the vitreous cavity. Am. J. Ophthalmol. 115, 770–774.
Mannermaa, E., Reinisalo, M., Ranta, V.P., Vellonen, K.S., Kokki, H., Saarikko, A., Kaarniranta, K., Urtti, A., 2010. Filter-cultured ARPE-19 cells as outer blood-retinal barrier model. Eur. J. Pharm. Sci. 40, 289–296.

Maurice, D., 2001. Review: practical issues in intravitreal drug delivery. J. Ocul. Pharmacol. Ther. 17, 393–401.
Maurice, D.M., Mishima, S., 1984. Ocular pharmacokinetics. In: Anonymous Pharmacology of the Eye. Springer-Verlag.
Meyer, C.H., Krohne, T.U., Holz, F.G., 2011. Intraocular pharmacokinetics after a single intravitreal injection of 1.5 mg versus 3.0 mg of bevacizumab in humans. Retina 31, 1877–1884.
Missel, P.J., 2012. Computer modeling for drug delivery. In: Thassu, D., Chader, G.J. (Eds.), Ocular Drug Delivery Systems, first ed. CRC Press, Taylor & Francis group, pp. 59–94.
Mochizuki, K., Torisaki, M., Yamashita, Y., Komatsu, M., Tanahashi, T., 1993. Intravitreal flomoxef sodium in rabbits. Ophthalmic Res. 25, 128–136.
Mochizuki, K., Yamashita, Y., Torisaki, M., Komatsu, M., Tanahashi, T., Kawasaki, K., 1992. Intraocular kinetics of ceftazidime (Modacin). Ophthalmic Res. 24, 150–154.
Moisseiev, E., Waisbourd, M., Ben-Artsi, E., Levinger, E., Barak, A., Daniels, T., Csaky, K., Loewenstein, A., Barequet, I.S., 2014. Pharmacokinetics of bevacizumab after topical and intravitreal administration in human eyes. Graefes Arch. Clin. Exp. Ophthalmol. 252, 331–337.
Morlet, N., Young, S., Naidoo, D., Graham, G., Coroneo, M.T., 1996. High dose intravitreal ganciclovir injection provides a prolonged therapeutic intraocular concentration. Br. J. Ophthalmol. 80, 214–216.
Nilsson, S.F.E., Alm, A., 2012. Determination of ocular blood flows with the microsphere method.. In: Anonymous Ocular Blood Flow. Springer.
Nomoto, H., Shiraga, F., Kuno, N., Kimura, E., Fujii, S., Shinomiya, K., Nugent, A.K., Hirooka, K., Baba, T., 2009. Pharmacokinetics of bevacizumab after topical, subconjunctival, and intravitreal administration in rabbits. Invest. Ophthalmol. Vis. Sci. 50, 4807–4813.
Obach, R.S., Lombardo, F., Waters, N.J., 2008. Trend analysis of a database of intravenous pharmacokinetic parameters in humans for 670 drug compounds. Drug Metab. Dispos. 36, 1385–1405.
Panda-Jonas, S., Jonas, J.B., Jakobczyk, M., Schneider, U., 1994. Retinal photoreceptor count, retinal surface area, and optic disc size in normal human eyes. Ophthalmology 101, 519–523.
Pearson, P.A., Hainsworth, D.P., Ashton, P., 1993. Clearance and distribution of ciprofloxacin after intravitreal injection. Retina 13, 326–330.
Pflugfelder, S.C., Hernandez, E., Fliesler, S.J., Alvarez, J., Pflugfelder, M.E., Forster, R.K., 1987. Intravitreal vancomycin. Retinal toxicity, clearance, and interaction with gentamicin. Arch. Ophthalmol. 105, 831–837.
Pitkanen, L., Ranta, V.P., Moilanen, H., Urtti, A., 2005. Permeability of retinal pigment epithelium: effects of permeant molecular weight and lipophilicity. Invest. Ophthalmol. Vis. Sci. 46, 641–646.
Pitkanen, L., Ruponen, M., Nieminen, J., Urtti, A., 2003. Vitreous is a barrier in nonviral gene transfer by cationic lipids and polymers. Pharm. Res. 20, 576–583.
Quinn, R.H., Miller, S.S., 1992. Ion transport mechanisms in native human retinal pigment epithelium. Invest. Ophthalmol. Vis. Sci. 33, 3513–3527.
Raju, B., Thiagarajan, G., Das, T., Hyderabad Endophthalmitis Research Group, 2004. Modified high-performance liquid chromatography technique for detection of vancomycin in human vitreous. Ophthalmic Res. 36, 55–61.
Reichenbach, A., Ziegert, M., Schnitzer, J., Pritz-Hohmeier, S., Schaaf, P., Schober, W., Schneider, H., 1994. Development of the rabbit retina. V. The question of 'columnar units'. Brain Res. Dev. Brain Res. 79, 72–84.
Roh, S., Weiter, J.J., Duker, J.S., 2006. Ocular circulation. In: Anonymous Duane's Ophthalmology on CD-ROM, 2006 ed. Lippincott Williams & Wilkins. pp. (Chapter 5).
Rowe-Rendleman, C.L., Durazo, S.A., Kompella, U.B., Rittenhouse, K.D., Di Polo, A., Weiner, A.L., Grossniklaus, H.E., Naash, M.I., Lewin, A.S., Horsager, A., Edelhauser, H.F., 2014. Drug and gene delivery to the back of the eye: from bench to bedside. Invest. Ophthalmol. Vis. Sci. 55, 2714–2730.
Ruby, A.J., Williams, G.A., Blumenkranz, M.S., 2006. Vitreous humor. In: Anonymous. Lippincott Williams & Wilkins.
Sanford, M., 2013. Fluocinolone acetonide intravitreal implant (IluvienÂ®). Drugs 73, 187–193.
Schoenwald, R.D., 2003. Ocular pharmacokinetics and pharmacodynamics. In: Mitra, A.K. (Ed.), Ophthalmic Drug Delivery Systems, pp. 135–179.
Sebag, J., Tang, M., Brown, S., Sadun, A.A., Charles, M.A., 1994. Effects of pentoxifylline on choroidal blood flow in nonproliferative diabetic retinopathy. Angiology 45, 429–433.
Severn, P.S., Hamilton, R., 2015. The incidence of serious complications associated with intravitreal therapy in a quaternary ARMD service (2008-2014). Eye (Lond) 29, 150.
Shen, Y.C., Wang, M.Y., Wang, C.Y., Tsai, T.C., Tsai, H.Y., Lee, Y.F., Wei, L.C., 2007. Clearance of intravitreal voriconazole. Invest. Ophthalmol. Vis. Sci. 48, 2238–2241.
Stewart, M.W., Rosenfeld, P.J., 2008. Predicted biological activity of intravitreal VEGF Trap. Br. J. Ophthalmol. 92, 667–668.
Tan, L.E., Orilla, W., Hughes, P.M., Tsai, S., Burke, J.A., Wilson, C.G., 2011. Effects of vitreous liquefaction on the intravitreal distribution of sodium fluorescein, fluorescein dextran, and fluorescent microparticles. Invest. Ophthalmol. Vis. Sci. 52, 1111–1118.
Taskintuna, I., Rahhal, F.M., Capparelli, E.V., Cundy, K.C., Freeman, W.R., 1998. Intravitreal and plasma cidofovir concentrations after intravitreal and intravenous administration in AIDS patients with cytomegalovirus retinitis. J. Ocul. Pharmacol. Ther. 14, 147–151.
Totan, Y., Guler, E., Guragac, F.B., 2015. Dexamethasone intravitreal implant for chronic diabetic macular Edema resistant to intravitreal bevacizumab treatment. Curr. Eye Res. 1–7.
Urtti, A., 2006. Challenges and obstacles of ocular pharmacokinetics and drug delivery. Adv. Drug Deliv. Rev. 58, 1131–1135.
Vellonen, K.S., Malinen, M., Mannermaa, E., Subrizi, A., Toropainen, E., Lou, Y.R., Kidron, H., Yliperttula, M., Urtti, A., 2014. A critical assessment of in vitro tissue models for ADME and drug delivery. J. Control. Release 190, 94–114.
Wiederholt, M., Kossendrup, D., Schulz, W., Hoffmann, F., 1986. Pharmacokinetic of topical cyclosporin A in the rabbit eye. Invest. Ophthalmol. Vis. Sci. 27, 519–524.
Wingard Jr., L.B., Zuravleff, J.J., Doft, B.H., Berk, L., Rinkoff, J., 1989. Intraocular distribution of intravitreally administered amphotericin B in normal and vitrectomized eyes. Invest. Ophthalmol. Vis. Sci. 30, 2184–2189.
Wu, C.D., Müller, H.K., Hockwin, O., Noll, E., 1970. Determination of the wet and dry weight of Iris, ciliary body and choroid in man and in different animal species. Ophthalmic Res. 1, 124.
Xu, J., Heys, J.J., Barocas, V.H., Randolph, T.W., 2000. Permeability and diffusion in vitreous humor: implications for drug delivery. Pharm. Res. 17, 664–669.
Xu, Q., Boylan, N.J., Suk, J.S., Wang, Y., Nance, E.A., Yang, J., McDonnell, P.J., Cone, R.A., Duh, E.J., Hanes, J., 2013. Nanoparticle diffusion in, and microrheology of, the bovine vitreous ex vivo. J. Control. Release 167, 76–84.
Zamudio, A.C., Candia, O.A., 2011. Interaction between mechanical and osmotic forces in the isolated rabbit lens. Exp. Eye Res. 93, 798–803.
Zhang, K., Zhang, L., Weinreb, R.N., 2012. Ophthalmic drug discovery: novel targets and mechanisms for retinal diseases and glaucoma. Nat. Rev. Drug Discov. 11, 541–559.
Zhu, Q., Ziemssen, F., Henke-Fahle, S., Tatar, O., Szurman, P., Aisenbrey, S., Schneiderhan-Marra, N., Xu, X., Tubingen Bevacizumab Study Group, Grisanti, S., 2008. Vitreous levels of bevacizumab and vascular endothelial growth factor-A in patients with choroidal neovascularization. Ophthalmology 115, 1750–1755, 1755.e1.